

Interaction of Cocos and Rivera Plates with the Upper Mantle Transition Zone Underneath Central Mexico

Xyoli Pérez-Campos^{1,2}, Robert W. Clayton²,

¹ *Departamento de Sismología, Instituto de Geofísica, Universidad Nacional Autónoma de México, Ciudad Universitaria, Coyoacán; Mexico, D. F. 04510, MEXICO*

² *Seismological Laboratory, California Institute of Technology, Pasadena, CA 91125, USA*

Supplementary Material

1 **Figure S1.** a) Number of RFs per station. The various networks are distinguished (MASE,
 2 VEOX, MARS, GGAP, CONA, SSN). The number in parenthesis corresponds to the total
 3 RFs obtained for each network. The inset shows the distribution for each network of the
 4 semblance percentage between the estimated Q component (convolution of RF and
 5 observed L component) and the original Q component. The numbers in brown denote the
 6 percentiles 5, 25, 50, 75 and 95. This shows that more than 50 % of our RFs, when
 7 convolved with the L component reproduce at least 82 % of the observed Q component. b)
 8 Noise levels. Color shaded areas correspond to the 90 % of the median noise curves for
 9 each network. Black lines denote the new high-noise model (continuous) and new low-
 10 noise model (dashed) by Peterson (1993). The gray region represents the bandwidth we
 11 used for the RFs (0.025 – 0.3 Hz). c) Stacked RFs by ray parameter. Left: Unfiltered. Right:
 12 They have been filtered between 0.025 and 0.3 Hz. $P410s$ (green arrows) and $P660s$
 13 (orange arrows) correspond to the theoretical arrival of the converted phase P to S at 410
 14 km depth and at 660 km depth, respectively.

Figure S2. Azimuthal gap per node. It represents the largest azimuthal gap per node. In general, most events come from the SE, SW and NW, having the largest azimuthal gaps to the Northeast. The white line delimits the area within the nodes have an azimuthal gap less than 180°.

Figure S3. a) Position of profiles. b) Profiles along the direction of the slab subduction (1-16). Profiles 2, 4, 9, and 14 are shown in Figure 3. Each RF shows the stack and its confidence interval. The brown areas correspond to the slab according to Yang *et al.* (2009) for profiles 1, 2, and 4, and to Husker & Davis (2009) for profile 9. Brown areas for profiles 5, 6, 7, 8, 10, and 11 denote our interpretation of the position of the slab, given similarities on the RFs with previous profiles. Brown areas in profiles 15 and 16 correspond to areas of cold material in tomography by Li *et al.* (2008) that might correspond to a broken-off slab. Green areas denote regions of complex RFs. Black dashed lines denote our interpretation for the 410 and the 660. c) Profiles longitudinal to the slab (a-d). Brown area in profile d corresponds to cold material in tomography by Li *et al.* (2008) that might correspond to a broken-off slab. Green areas denote regions of complex RFs. Black dashed lines denote our interpretation for the 410 and the 660.

References

Husker, A. & Davis, P.M., 2009. Tomography and thermal state of the Cocos plate subduction beneath Mexico City, *J. Geophys. Res.*, **114**, B04306, doi:10.1029/2008JB006039.

- 38 Li, C., van der Hilst, R.D., Engdahl, E.R. & Burdick, S., 2008. A new global model for P
39 wave speed variations in Earth's mantle, *Geochem. Geophys. Geosyst.*, **9**, Q05018,
40 doi:10.1029/2007GC001806.
- 41 Peterson, J. (1993). Observations and modelling of background seismic noise. Open-file
42 report 93-322. *US Geological Survey*, Albuquerque, New Mexico.
- 43 Yang, T., Grand, S.P., Wilson, D., Guzman-Speziale, M., Gomez-Gonzalez, J.M.,
44 Dominguez-Reyes, T. & Ni, J., 2009. Seismic structure beneath the Rivera subduction
45 zone from finite-frequency seismic tomography, *J. Geophys. Res.*, **114**, B01302,
46 doi:10.1029/2008JB005830.
- 47

Figure S1.

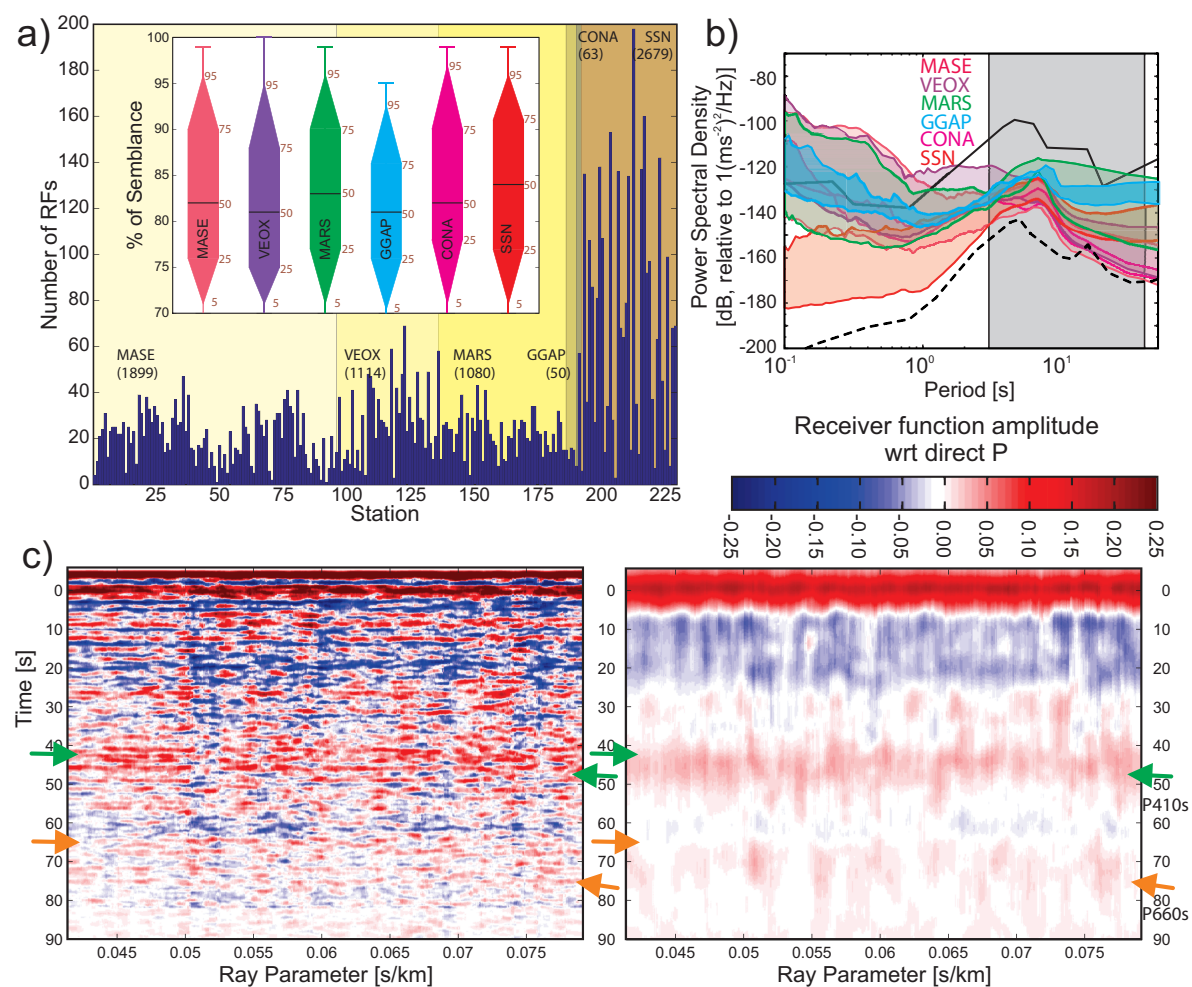


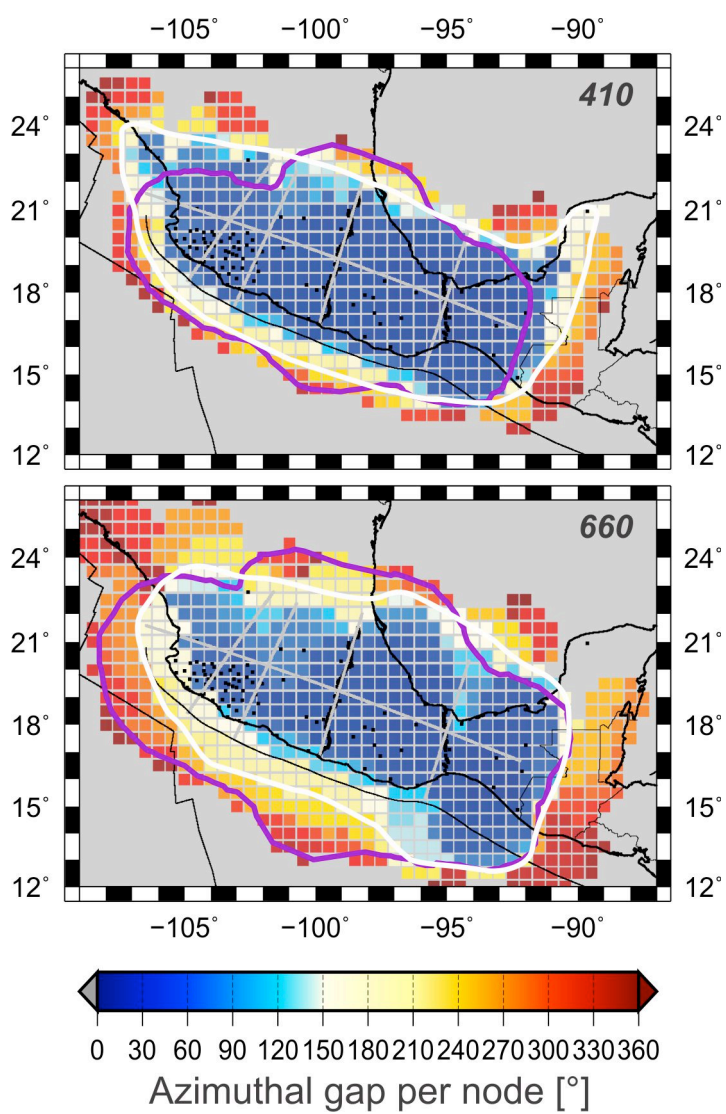
Figure S2.

Figure S3.

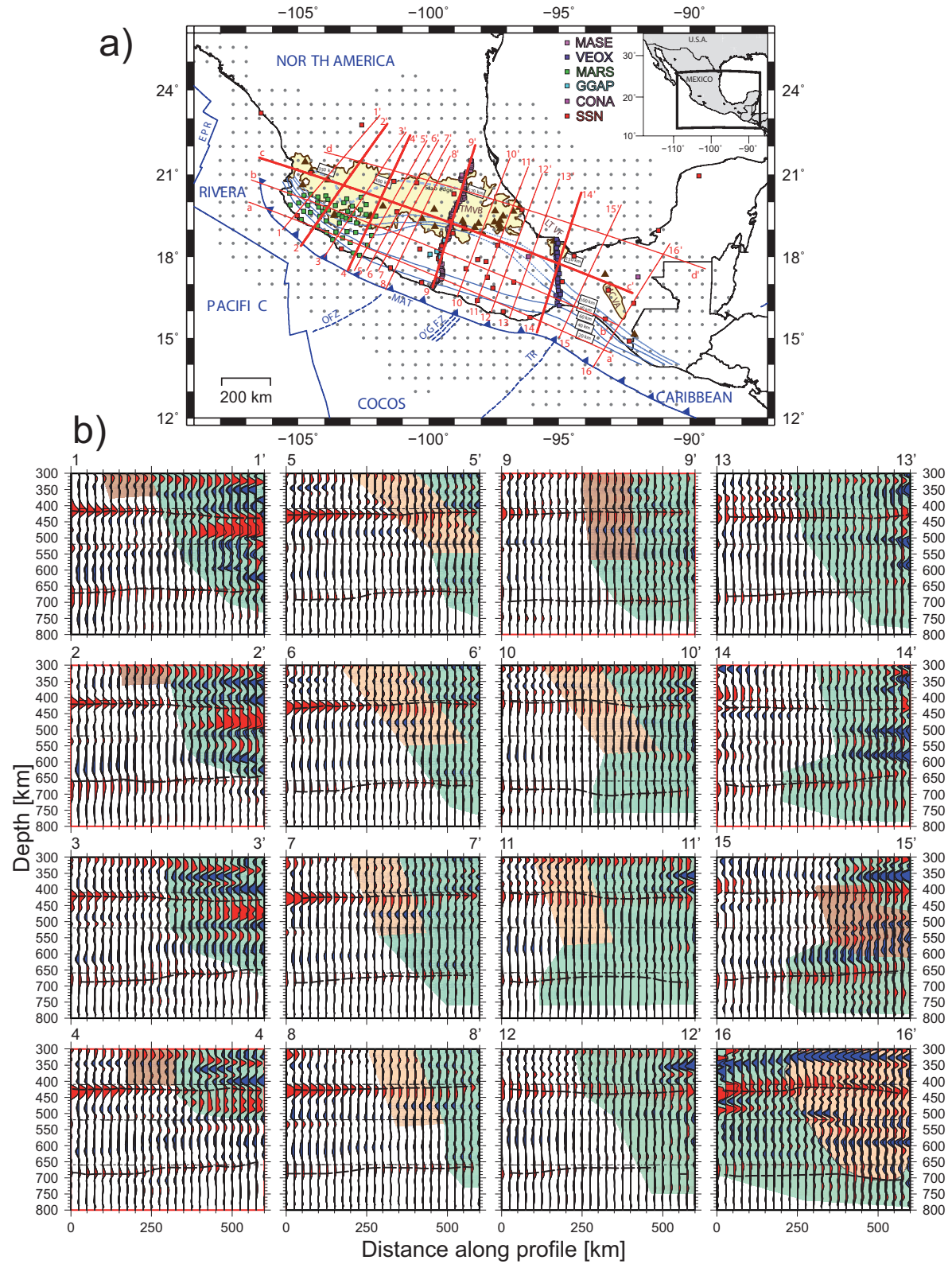


Figure S3. Continuation.